On-site LNG production at filling stations

ON-SITE LNG PRODUCTION AT FILLING STATIONS

M. A. Ancona*, M. Bianchi, L. Branchini, A. De Pascale, F. Melino
DIN – Alma Mater Studiorum, Viale del Risorgimento 2, 40136 Bologna, Italy

M. Mormile, M. Palella
Graf S.p.a. – Via Galileo Galilei 36, 41015 Nonantola (MO), Italy

*corresponding author: e-mail: maria.ancona2@unibo.it, phone: +39-051-2093320

ABSTRACT

In the next decades fossil fuels are expected to still play a fundamental role within the energy market, contemporarily to the increased exploitation of renewable energy sources. Among all fossil fuels, natural gas is predicted to be the key source to achieve the satisfaction of the forecasted increase in energy demand, due to its lower environmental impact. In particular, great attention is being paid on the transport sector where liquefied natural gas can be seen as an interesting opportunity. In this context, this paper aims to elaborate a novel solution for liquefied natural gas production directly at filling stations. With this purpose, in this work four different liquefaction process layouts will be proposed and analyzed, considering natural gas supply grid operating at middle pressure or at low pressure. The developed configurations will be analyzed by applying an in-house developed calculation model, which enables to define the physical conditions in each section of the process and the energy fluxes of the plant.

In order to define a configuration which allows to minimize the process' energy consumption, a parametric analysis has been carried out to evaluate and compare the performance of the proposed processes. With this purpose, several performance indicators have been defined and applied to the considered scenarios.

Keywords: Liquefied Natural Gas; small-scale production; filling station; energy performance evaluation; parametric analysis.

NOMENCLATURE

A	pressure losses coefficient [-]
c_P	specific heat at constant pressure [kJ/kgK]
e	total specific electric energy consumption [kJ/kg]
HR^*	heat rate [-]
k	heat capacity ratio [-]
LHV	lower heating value [kJ/kg]
LHV_R	fuel residual lower heating value [kJ/kg]
$\dot{m}$	mass flow rate [kg/s]
P	electric power [kW]
p	pressure [bar]
Q	thermal power [kW]
S	heat exchanger surface [m^2]
T	temperature [°C]
U	global thermal exchange coefficient [$kW/m^2 \cdot °C$]
x	quality [-]

Greek symbols

β	pressure ratio [-]
ε	heat exchanger effectiveness [-]
η	efficiency [-]
ρ	fuel degradation index [-]

Subscripts and Superscripts

1,…,18	process sections of main interest
el	electric
em	electro-mechanical
POL	polytropic
R	residual

ref	reference
tot	total

Acronyms

C1	Compression train #1
C2	Compression train #2
CNG	Compressed Natural Gas
EER	Energy Efficiency Ratio
HE	Heat Exchanger
LNG	Liquefied Natural Gas
NG	Natural Gas
TV	Throttle Valve

1. INTRODUCTION

In the last years, a sustainable energy production turn into a fundamental issue due to the forecasted increase in energy demand, with a predicted average rate of 0.9-1.6 % per year [1, 2]. Since its environmental impact is lower than other fossil fuels [2, 3], Natural Gas (NG) is expected to play a key role in the energy market for the years to come. In 2014, indeed, the International Energy Agency (IEA) estimated that – from 2014 to 2040 – the global demand of energy will grow by 37% and, contemporarily, the demand of NG will increase more than the 50% [2].
In transport sector, NG can be used either as Liquefied Natural Gas (LNG) or Compressed Natural Gas (CNG). However, LNG is preferable due to the lower required volume: compared to natural gas, indeed, the volume of LNG is 600 times inferior at ambient temperature, while the CNG volume is only 1% less of its original value [4]. On the other hand, if compared to diesel fuel, the LNG price results for about the 50% cheaper [5]. For these reasons, the employment of LNG will certainly increase in the next years and, in 2035, it is expected to account for the 15% of the total NG consumption [6].
At present, LNG is mainly produced in large-scale plants located close to the NG extraction sites. Here, the NG is treated after the extraction, in order to be purified from undesirable substances (*i.e.* acid gas, water, mercury, heavy hydrocarbon, etc.), and usually liquefied through of one of the following processes:

1. a cascade process, by means of Joule-Thompson valves and based on different pure refrigerants (usually three), working at different temperature levels [7-12];
2. a mixed refrigerant process, developed to decrease the amount of required equipment regarding to the cascade process. This liquefaction process is composed by a single cycle employing mixture of refrigerants (mainly nitrogen and hydrocarbons, such as methane, ethane and propane) [13-26];
3. an expander process, based on the use of expanders instead of Joule-Thompson valves [27-34].

On the other hand, small-scale LNG production facilities are currently rare and mainly realized in order to reduce the workload on gas reservoirs sites [35] or for offshore compact LNG production [36]; in particular, based on [37], the number is 12 in 2015. Furthermore, this kind of plant is not common at refueling stations. Relating to the liquefaction process for small-scale applications, at present the main applied technologies consist of N_2 expander cycle and single-mixed refrigerant process (SMR) [38, 39]. The SMR process efficiency strongly depends on the optimization of mixed refrigerant composition and on the ambient conditions [38] and the power consumption of this process is usually lower than the N_2 expander cycle one. On the other hand, the efficiency of the latter is almost independent of feed gas condition. Moreover, nitrogen is a nonreactive refrigerant, then the safety is greater [40]. Yuan et al. have studied a small-scale NG liquefaction process adopting single nitrogen expansion with the aim to minimize the unit energy consumption. They demonstrate that the system is compact, reliable and it shows a good adaptability to the feed gas condition [41]. In [42] a novel NG liquefaction process is presented: this process allows to liquefy, without energy consumption, part of NG employing the pressure exergy of the pipeline. However, the system efficiency depends on the pipeline pressure and if it is too low the process may not work [42]. Finally, Jokinen et al. presented a mathematical model for the optimization of a small-scale LNG supply chain [43], which is mainly focused on the device and parameters concerning the NG side. In particular, this solution is designed to be directly installed at the vehicle's filling stations, in this way the costs relative to the transport of LNG are avoided.

In this scenario, the idea of generating LNG directly at filling stations has been developed, in order to give a compact solution and to avoid the economic and environmental costs related to LNG transportation by ship, contemporarily promoting LNG as fuel in transport sector. Furthermore, with respect to the processes usually applied in small-scale applications, this study is aimed to the realization of simpler – and, as a consequence, less expensive – solutions that can be competitive in the future global energy scenario.

In particular, the proposed approach is thought as an alternative to the current habit of LNG filling stations, as it can be seen from Figure 1 (red dotted line), where the whole NG value chain – from the natural gas extraction to the final users – is summarized and presented. As it can be observed from the figure, the production of LNG at filling stations enables to eliminate the ship transportation, the secondary storage and the road transport of LNG: thus, even if a small-scale process presumably penalizes the conversion efficiency (with respect to large scale facilities), the environmental and energy related costs can be considerably reduced.

Obviously, the proposed idea can be seen not only as an alternative to the LNG production at the extraction sites, but also in addition to this habit: since the existing LNG plants are expected to be not enough to meet the increasing global need, in the next years the number of LNG production plants is predicted to significantly raise.

In Figure 2, the current global liquefaction plants are presented as function of their production capacity (expressed in MTPA-Mega Tons Per Annum), revised and improved regarding to the Author's outlook previously presented in [44]. From the figure it can be noted that the majority of the liquefaction facilities has a production capacity over 1 MTPA (that is the lower capacity limit for large-scale plants [45]), while only few plants can be classified as small-scale facilities.

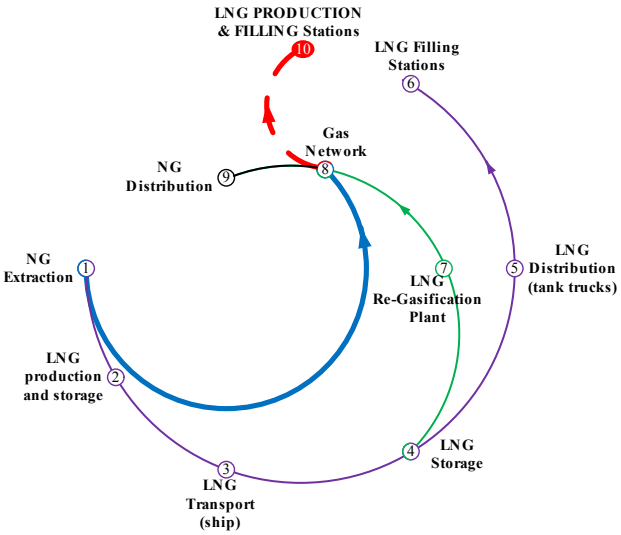

Figure 1 – NG value chain from extraction to final users.

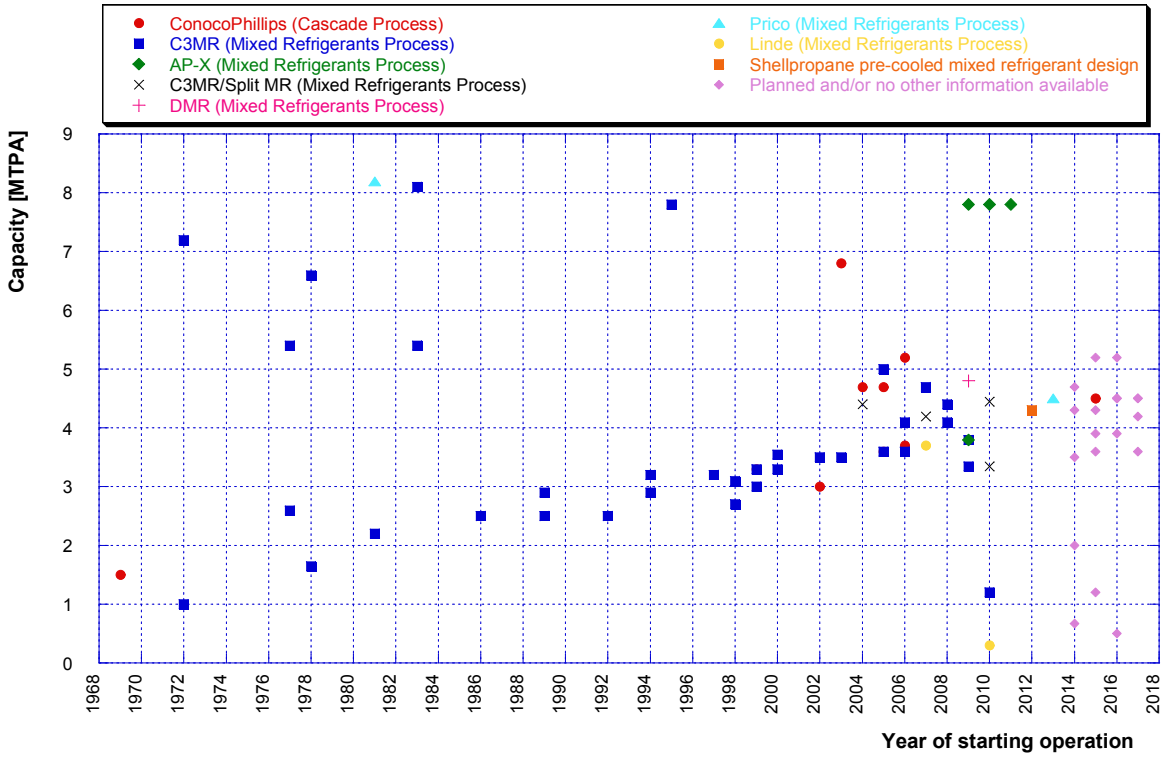

Figure 2 – Global LNG production plants and LNG production capacity [45, 46].

Hence, the aim of the paper is the definition of a liquefaction process for small-scale LNG production, with a parametric analysis carried out both to minimize the energy consumption and to limit operation and investment costs. Four possible configurations for the liquefaction plant will be presented, analyzed and discussed in the following paragraphs by applying an in-house developed calculation model and by considering several performance parameters. In more detail, two of the developed solutions consider a medium pressure NG grid supply: the difference between these two cases stands in the liquefaction process (provided respectively by a throttle valve or by a turbo-expander). The other two configurations, instead, consider a low pressure NG grid supply and differ for the storage pressure. The results obtained from the here presented analysis led to the realization of a prototype, owned by Ferrari Technology, being the basis for future evolutions.

2. REFERENCE CASE

Case MP1 – Medium Pressure NG grid and Joule-Thompson liquefaction process

The first layout considered for the analysis – shown in Figure 3 – is conceived to produce LNG with an isenthalpic Joule-Thompson process from a middle pressure natural gas stream. This layout has been developed by Authors in [44], starting from a double Joule-Thompson configuration [47], with the aim to both realize a simpler and less expensive solution and reduce the energy consumption. The configuration presented in Figure 3 is the result of an analysis – in terms of compression trains configuration and heat exchanger position – aimed to the minimization of the process energy consumption

As it can be seen in Figure 3, the configuration is based on two different lines: a primary line, to produce the liquid fraction (LNG with low pressure and temperature, to be sent to the storage tank), and a secondary line for the recovery, recompression and recirculation of the residual NG vapor fraction. More in detail, the natural gas hailing from the distribution grid (section 1), mixed with a recirculation stream from the secondary line (18), is cooled in the heat exchanger HE 3 before entering into the first compression train C1 (3), where the pressure is increased reaching its maximum value (7). After the compression C1, the NG stream is then cooled in the heat exchangers HE 2 (section 8) and HE 1 (section 9) and the LNG is produced by the Joule-Thomson valve TV (section 10). The liquid fraction (11) is finally separated in the flash tank and sent to the storage tank, while the vapor fraction (12) is recirculated and compressed in the compression train C2 (18) before the mixing with the NG supply stream.

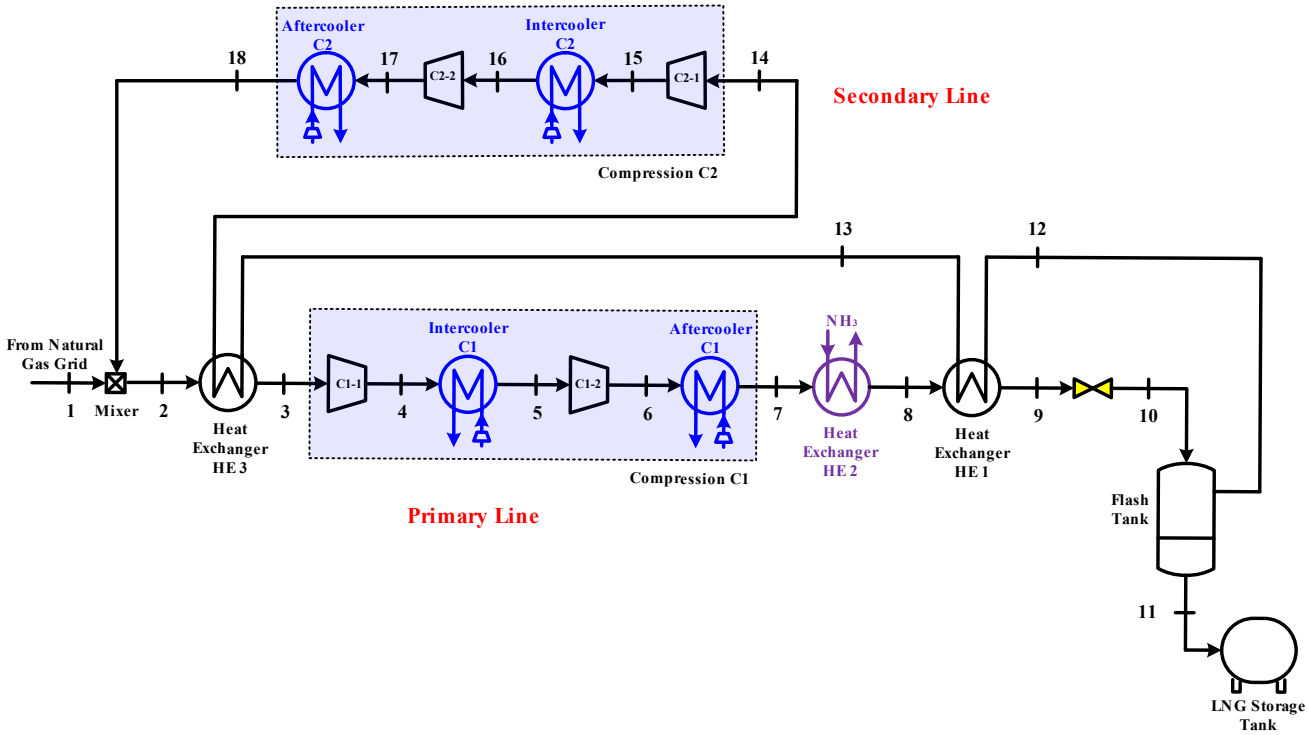

Figure 3 – Layout for the liquefied natural gas production process by means of Joule-Thompson valve (Case MP1).

It must be pointed out that the low temperature vapor fraction coming from the flash tank provides for the cooling effect in the heat exchangers HE 1 and HE 3 before entering into the compression train C2. On the other hand, the cooling effect of the heat exchanger HE 2 is provided by a compression chiller working with ammonia (NH_3) refrigeration fluid. Moreover, both the compression trains have been initially supposed to be inter-cooled and after-cooled with air cooled heat exchangers.

Based on the presented layout, a parametric analysis has been carried out in [39] involving the maximum pressure of the cycle (p_7, ranging from 200 bar to 300 bar), the LNG storage pressure (p_{10}, ranging from 3 bar to 15 bar) and the chilling temperature (T_8, ranging between -20°C and -50°C). With this sensitivity analysis, the optimum values – within the considered ranges – for the before mentioned cycle's key parameters have been found and fixed, as presented in Table 1 along with the remaining main input of the process.

In order to justify the final choice of the investigated parameters' values, in Figure 4 and in Figure 5 (both already presented in [44]) are respectively shown the trends of the specific electric energy consumption of the process (considered in the following analysis as one of the main performance indicators) and the quality achieved at the end of the Joule-Thompson valve, as function of the maximum pressure of the cycle and of the LNG storage pressure. As it can be seen from the presented figures, the higher the maximum pressure of the cycle (p_7), the lower the quality at the outlet of the Joule-Thompson valve, while a weak effect can be seen on the specific electric energy consumption. On the other hand, for fixed p_7, an increase in the throttle valve outlet pressure (p_{10}) produces the decrease of the quality at the end of the Joule-Thompson isenthalpic process and contemporarily a remarkable decrease in the specific electric energy consumption of the process. This evidence is due to the decrease in the mass flow rate required to produce 1 kg/s of LNG (fixed parameter, see Table 1), as a direct consequence of the quality decrease [44].

Since the results of the parametric analysis show that – in the considered range – the preferable value for the storage tank pressure is 15 bar, a further discussion about this parameter should be made. In fact, this value may seem quite high for a LNG vehicle: however, several producers already implement in their LNG vehicles storage tanks with a maximum allowed pressure comparable with the considered one. In particular, SCANIA [48] realizes LNG driven trucks able to operate with pressures until 16 bar. Furthermore, models D650 and D500 by HVM [49] – an Italian company that is one of the leaders in European market for the construction and repair of transportable cryogenic vessel – allow a maximum working pressure equal to 16 bar. Obviously, with respect to ambient pressure storage systems, major efforts have to be made for the vehicle safety in order to guarantee the operation with high pressure storage, but the technology is already available. In fact, it should be pointed out that these technologies, at present, are able to resist up to 16 bar, but are normally operated with lower pressure values: as a consequence, the possibility of boil-off gas formation becomes an important issue for the implementation of the proposed solution [50].

Finally, from the vehicles point of view, the introduction of a pressurized tank entails an additional load, which may decrease the transport efficiency.

Table 1 – Main parameters of the Joule-Thompson valve related liquefying process.

T_1	[°C]	20
p_1	[bar]	30
T_3	[°C]	-5
P_7	[bar]	200
p_{18}	[bar]	30
$\eta_{POL,C}$ (each compression)	[-]	0.76(*)
$\eta_{em,C}$ (each compressor)	[-]	0.90
HE1 effectiveness (ε)	[-]	0.70
p_{10}	[bar]	15
$\dot{m}_{LNG}$	[kg/s]	1
EER of the HE2 chiller	[-]	1.1
T_8	[°C]	-50
$T_5 = T_7 = T_{16}$	[°C]	30
Pressure losses (each HE)	[%]	2
Minimum pinch (each HE)	[°C]	20

(*) Value of polytropic efficiency corresponding to a set of existing commercial machines.

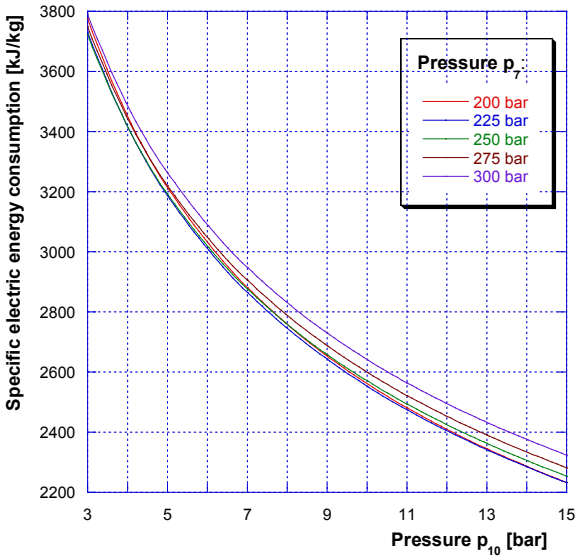

Figure 4 – Specific electric energy consumption as function of the LNG storage pressure p_{10} and of the maximum pressure of the cycle p_7 [44].

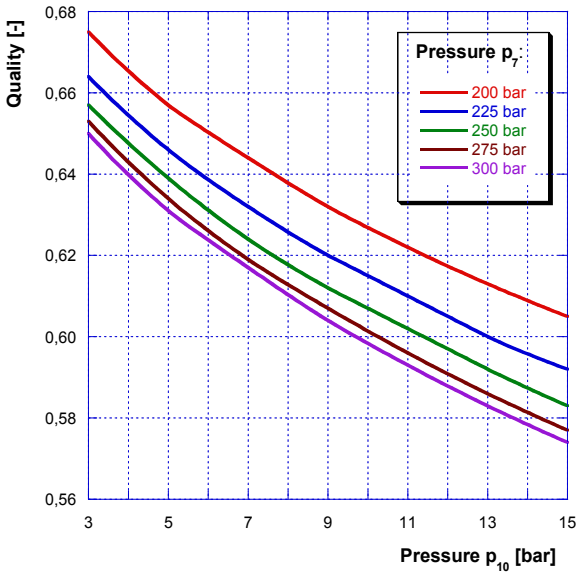

Figure 5 – Quality achieved at the end of the Joule-Thompson process as function of the LNG storage pressure p_{10} and of the maximum pressure of the cycle p_7 [44].

Furthermore, one of the other results of the analysis presented in [44] indicates that the intercooling of the compression train C2 is not necessary, thus only the after-cooler has been finally considered for C2 (for completeness in Figure 3 both the inter-cooler and the after-cooler of the compressor C2 have been shown).
In this study, this before-developed configuration has been set as Reference Case to optimize the process, as presented and discussed in the following paragraphs.

3. CASE STUDIES

Case MP2 – Medium Pressure NG grid and turbo-expander liquefaction process

The second analyzed layout – presented in Figure 6 – considers a turbo-expander instead of the Joule-Thompson throttle valve, in order to further improve the performance of the process and to reduce the electric energy consumption. The remaining part of the layout is not modified with respect to the Case 1. An isentropic efficiency equal to the 70% [51] has been considered for the turbo-expansion process (see Table 2 for the main parameters of the process).

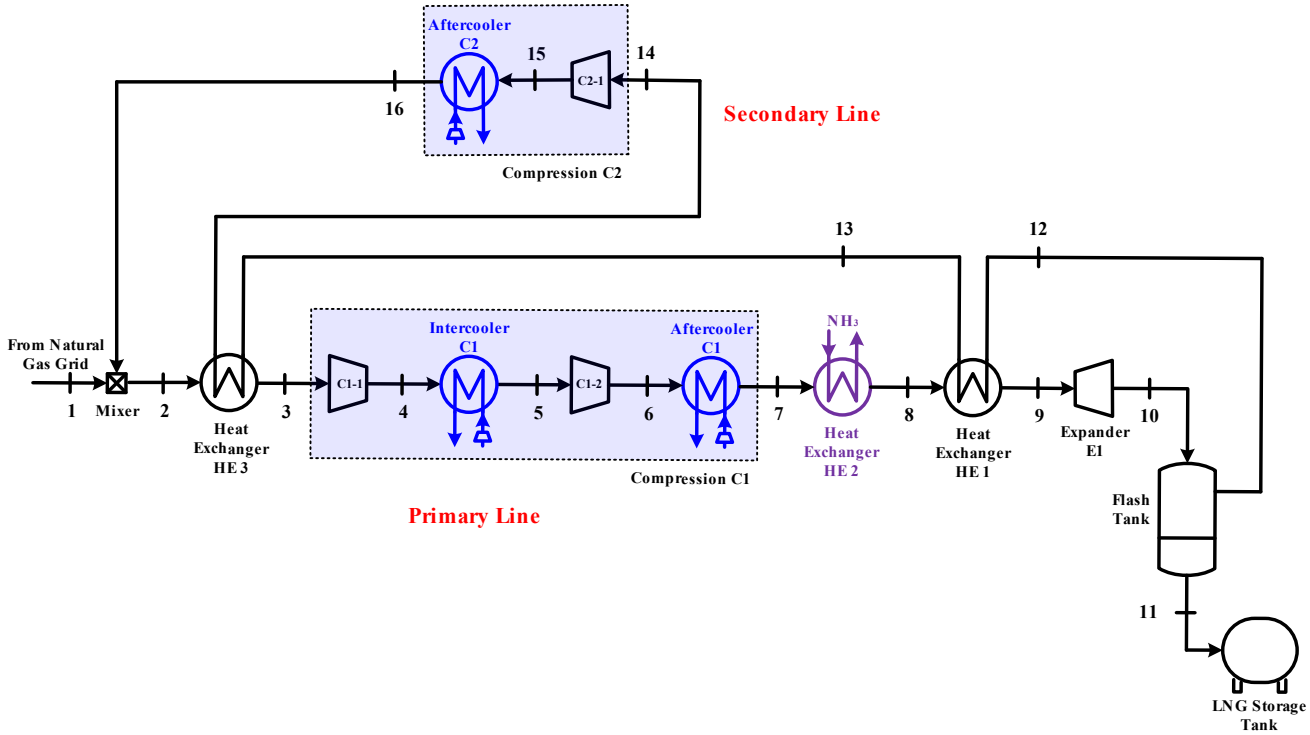

Figure 6 – LNG production layout with turbo-expander (Case MP2).

Table 2 – Main parameters of the turbo-expander related liquefying process.

T_1	[°C]	20
p_1	[bar]	30
T_3	[°C]	-5
P_7	[bar]	200
p_{16}	[bar]	30
$\eta_{POL,C}$ (each compression)	[-]	0.76(*)
$\eta_{em,C}$ (each compressor)	[-]	0.90
HE1 effectiveness (ε)	[-]	0.70
p_{10}	[bar]	15
$\dot{m}_{LNG}$	[kg/s]	1
EER of the HE2 chiller	[-]	1.1
T_8	[°C]	-50
$T_5 = T_7 = T_{16}$	[°C]	30
Pressure losses (each HE)	[%]	2
Expander isentropic efficiency	[-]	0.70

(*) Value of polytropic efficiency corresponding to a set of existing commercial machines.

Cases LP1 and LP2 - Low pressure NG grid

In this study also the case of producing LNG from natural gas hailed by a low pressure NG grid has been considered. This case is introduced in order to simplify the process' layout and to realize an easy solution to be connected directly to the NG national grid's low pressure terminals. For this reason and in order to reduce the plant's investment costs, the presented layout do not consider the turbo-expander, but the liquefaction is provided again by means of the throttle valve. Furthermore, this study has been carried out in collaboration with Ferrari Technology Company, aiming for the realization of a prototype of this system.

For this case, two possible configurations, with different LNG storage pressures, are proposed: in the first one, Case LP1 presented in Figure 7, the secondary line of the process doesn't necessitate of the compression train C2, but – in order to maintain the same pressure of the previous cases for the produced LNG (*i.e.* 15 bar) – a further isenthalpic expansion (from section 12 to section 13 in Figure 7) is necessary to mix the residual vapor fraction exiting from the flash tank with the NG supplied from the network. The second proposed configuration (Case LP2 shown in Figure 8), instead, considers a production of LNG at the same pressure of the NG grid (obviously increased to overcome the pressure losses between the flash tank and the mixer). For this reason no Joule-Thompson valve or compressor are required in the secondary line.

The main assumptions for the carried-out simulations are presented in Table 3.

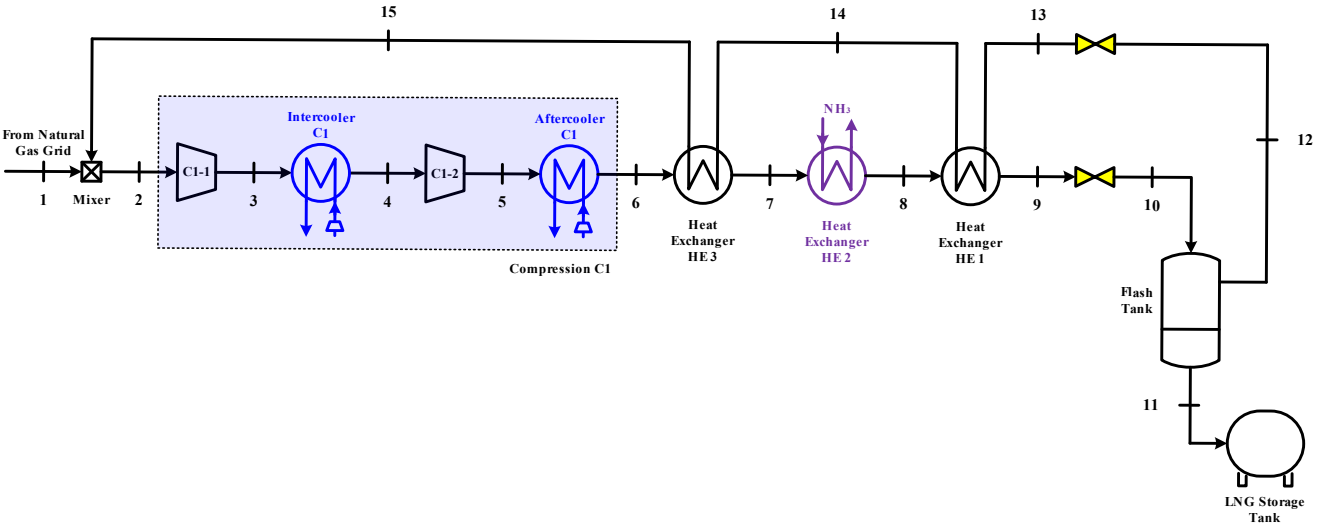

Figure 7 – Low pressure hailing grid LNG production layout (Case LP1).

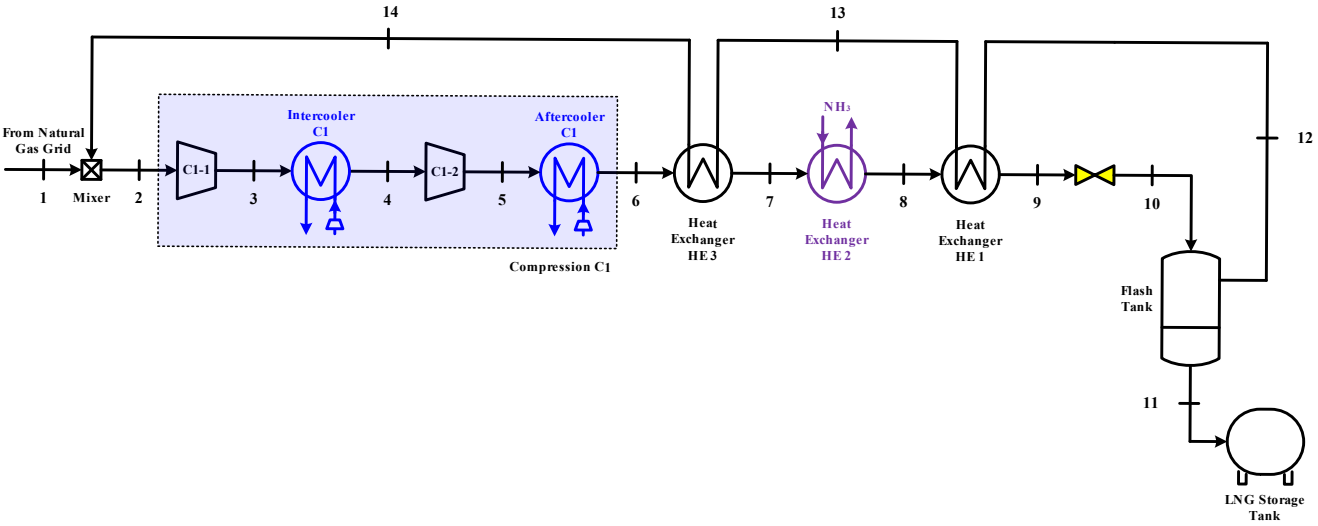

Figure 8 – Low pressure hailing grid LNG production layout with low pressure LNG storage (Case LP2).

Table 3 – Input of the low pressure NG grid related liquefying process.

		Case LP1	Case LP2
T_1	[°C]	20	20
p_1	[bar]	3	3
P_6	[bar]	200	200
$\eta_{POL,C1}$	[-]	0.76(*)	0.76(*)
$\eta_{em,C1}$	[-]	0.90	0.90
HE1 effectiveness (ε)	[-]	0.70	0.70
p_{10}	[bar]	15	3.12
$\dot{m}_{LNG}$	[kg/s]	1	1
EER of the HE2 chiller	[-]	1.1	1.1
T_8	[°C]	-50	-50
$T_4 = T_6$	[°C]	30	30
Pressure losses (each HE)	[%]	2	2

(*) Value of polytropic efficiency corresponding to a set of existing commercial machines.

4. CALCULATION MODEL AND ASSUMPTIONS

Calculation model

The thermodynamic analysis of the LNG production processes have been carried out with a calculation model, specifically developed in Visual Basic for Application (VBA) environment. This calculation model, on the basis of an iterative resolution of mass and energy balances for each component of the plant, enables to evaluate the physical conditions in each section of the layout and the process energy fluxes. Furthermore, the FluidProp [52] database is implemented into the calculation code for the thermodynamic properties of the NG streams.

In greater detail, the developed model requires the following input data (see Figure 3 for the sections identification numbers):

- the supply NG composition, pressure and temperature (section 1);
- the HE 3 heat exchanger effectiveness or, alternatively, the temperature in the section 3;
- the outlet pressures of the compressors C1 and C2 (*i.e.* the pressure ratio);
- the polytropic (η_{POL}) and electro-mechanic (η_{em}) efficiencies of the compressors C1 and C2;
- the effectiveness (ε) of the heat exchanger HE 1;
- the throttle valve's outlet pressure (p_{10});
- the LNG mass flow rate to the storage tank ($\dot{m}_{LNG}$);
- the Energy Efficiency Ratio (EER) of the compression chiller and the desired temperature in the section 8;
- the inter-cooling and after-cooling temperatures;
- the pressure losses for each heat exchanger of the layout.

Then, on the basis of these input, the following outputs are given:

- physical conditions (pressure, temperature, enthalpy and quality) and mass flow rate in each section of the process;
- thermal energy exchanged by each heat exchanger;
- specific work and electric power required by each compressor;
- electric power required by the compression chiller;
- specific work and electric power generated by the expander (when present).

Hypothesis and assumptions

In addition to the input parameters, given in the previous section for each case, the developed calculation model requires some other assumptions as described in the following of this paragraph.

First of all, the natural gas composition of the stream coming from the grid must be specified. For the sake of simplicity, the analysis has been developed by considering 100% of CH_4 for the NG composition. This simplifying hypothesis has been assumed starting from typical natural gas composition [53] and testing the weak effect of the other components (water, carbon dioxide, hydrocarbons, etc.). In more detail, the natural gas coming from the Italian national grid is completely lacking of H_2O [53], due to the removal directly at the extraction sites. Similarly, the carbon dioxide is usually separated after the extraction by means of absorption processes, cryogenic distillation or selective membrane systems [54].

The effect of other possible components (such as ethane, propane and iso-butane) has been finally taken into account only monitoring the process temperatures (*i.e.* considering the process sections of components' condensation).

Furthermore, as already explained, both the compression trains have been initially supposed to be inter-cooled and after-cooled with air cooled heat exchangers. Relating to the compression train C1, it must be considered that the presence of inter-cooling and after-cooling steps implies the split of the total required pressure ratio ($\beta_{tot,C1}$) between the two compression stages. In this study, the minimum compression specific work criterion – including the pressure losses due to the inter-cooling and the after-cooling heat exchangers – has been applied. Thus, relating to the layout of Case MP1 (see Figure 3) for the considered sections numbers, for the compression train C1 stands:

$$\beta_{1,C1} = \frac{p_4}{p_3} = \frac{1}{A}\sqrt{\beta_{C1}}\sqrt{\left(\frac{T_5}{T_3}\right)^{\frac{k}{k-1}\eta_{POL}}} \qquad [E1]$$

$$\beta_{2,C1} = \frac{\beta_{tot,C1}}{A\beta_{1,C1}} \qquad [E2]$$

where:

- $\beta_{C1} = {p_7}/{p_3}$ is the external pressure ratio of the compression train C1;

- $\beta_{tot,C1} = {p_6}/{p_3}$;
- the coefficient A has been introduced to consider the pressure losses through the inter-cooler and the after-cooler exchangers and it is defined as $A = {p_5}/{p_4} = {p_7}/{p_6}$.

For the sake of simplicity, in this study it is assumed that the same percentage pressure drop (equal to the 2%, see Tables 1, 2 and 3) occurs throughout each of the heat exchangers, as it can be easily understood from the definition of the coefficient A (then A is equal to 0.98).
The analytical demonstration of the above-written equations is presented in [44].
Relating to the compression train C2, instead, the same criterion has been utilized at the beginning of the analysis to split the total pressure ratio between the two stages. Since the results presented in this study refer to the optimized cases without the need of the inter-cooling, the expressions of the pressure ratios for the compression train C2 are not presented here.

Performance indicators

With the aim to evaluate and compare the performances of the proposed processes, three different indexes have been defined in [44] as follows:

1. *total specific electric energy consumption* (*e*), expressed in [kJ/kg] and defined as:

$$e = \frac{P_{el}}{\dot{m}_{LNG}} \quad \text{[E3]}$$

being P_{el} [kW] the electric power required by the whole liquefaction process and $\dot{m}_{LNG}$ [kg/s] the LNG produced mass flow rate;

2. *fuel residual lower heating value* (LHV_R), expressed in [kJ/kg] and defined as:

$$LHV_R = LHV - \frac{e}{\eta_{el,ref}} = LHV - e \cdot HR^*_{ref} \quad \text{[E4]}$$

where: $\eta_{el,ref}$ [-] is the *reference electrical efficiency* that allows to convert the total specific electric energy consumption (*e*) into the corresponding specific primary energy introduced with fuel; HR^*_{ref} [-] is the *reference heat rate* defined as $HR^*_{ref} = {1}/{\eta_{el,ref}}$; LHV, expressed in [kJ/kg], is the Lower Heating Value of the fuel.

3. *fuel degradation index* (ρ), that is a non-dimensional parameter defined as:

$$\rho = \frac{LHV_R}{LHV} = \frac{LHV - e \cdot HR^*_{ref}}{LHV} = 1 - e \cdot \frac{HR^*_{ref}}{LHV} \quad \text{[E5]}$$

representing the fuel loss in energy content due to the liquefaction transformation.
The first of the proposed performance indicators, namely the total specific electric energy consumption (*e*), is obviously essential in order to evaluate and compare the electricity consumption (and consequently the related costs) of the different proposed configurations. On the other hand, the last two indexes are essential for a thermodynamic evaluation on the fuel obtained after the liquefaction process. As well known, indeed, the thermodynamic properties of the LNG are not the same as the ones of the NG which it is derived from: in particular, the liquefaction transformation produces a decrease in the LHV, that means a degradation of the fuel with respect to its starting condition.
In the present study, these indicators have been applied to the different proposed layout in order to estimate and compare the performance of the liquefaction processes.

5. RESULTS AND DISCUSSION

The thermodynamic diagrams *Log P-h* of the liquefaction process' transformations are presented in Figure 9 and in Figure 10, respectively for the middle pressure and for the low pressure supply grid cases. In particular, the quality achieved at the end of the liquefaction process (namely the quality at the flash tank) – which is linked to the temperature and to the pressure

achieved at the outlet of the heat exchanger HE 1 – is a fundamental parameter to evaluate the performance of the process. Being fixed the mass flow rate of LNG to be sent to the storage tank (1 kg/s), indeed, the achieved quality has a direct impact on the mass flow rate circulating on the primary and on the secondary lines and, consequently, also on the electric energy consumption of the compressors. More in detail, the lower is the quality the lower is the mass flow rate required to produce 1 kg/s of LNG, thus a benefit on the electric consumption can be reached (being fixed all the other cycle's parameters).
As it can be seen from the diagrams in Figure 9 and in Figure 10, the Case MP2 allows to achieve the lowest quality (equal to 0.403) compared to the other presented configurations. The quality achievable with the Case MP1 (0.510) and with the Case LP1 (0.498), indeed, from the figures results clearly closer to the saturation vapor curve than Case MP2. Relating to the Case LP2, instead, from the diagram the increase in the quality results less evident due to the different pressure reached at the end of the expansion process, but the analysis shows for this configuration a quality equal to 0.601. As already explained, in order to realize an easy and not expensive solution, in this study the turbo-expander has not been considered in the case of low pressure supply grid. However, future works will investigate also this possibility due to the expected achievable improvement of the performance.
For completeness, the physical conditions (pressure, temperature and quality) in each section of the process are reported in Appendix A, along with the circulating mass flow rates.

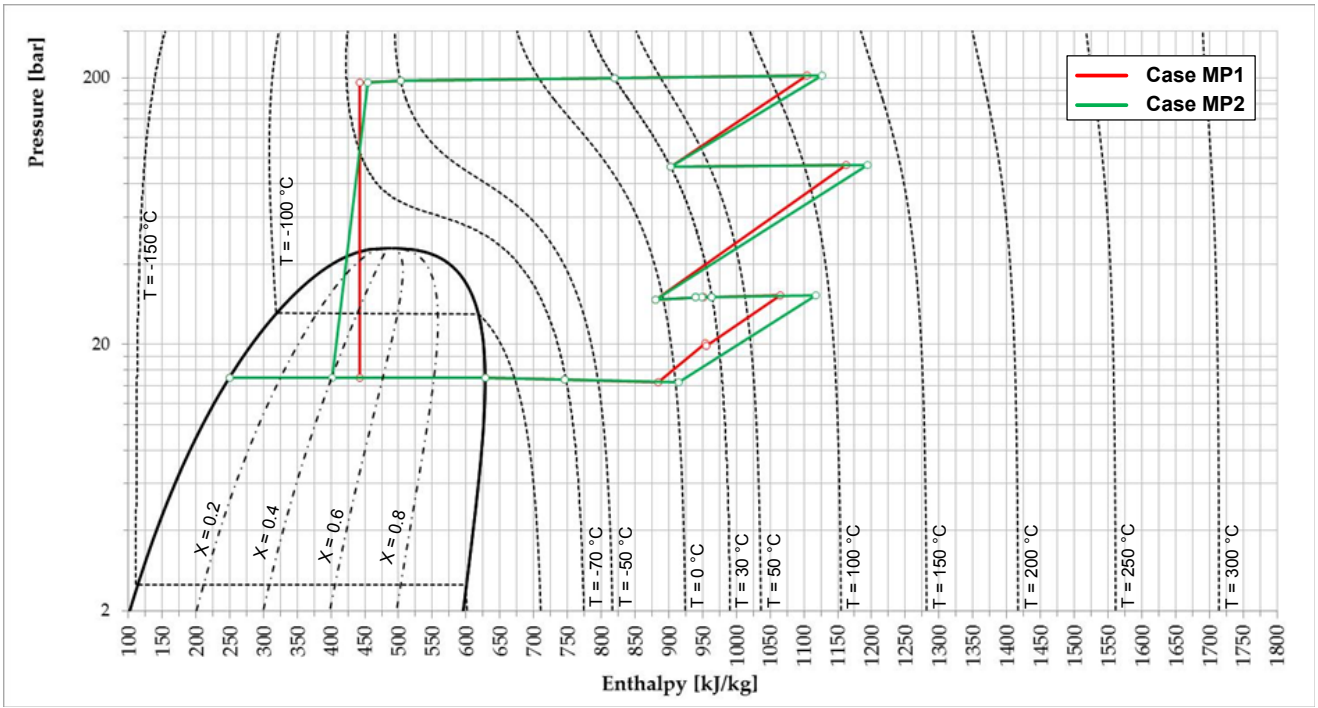

Figure 9 – Thermodynamic diagram of the process obtained for the Case MP1 (red line) and for the Case MP2 (in green).

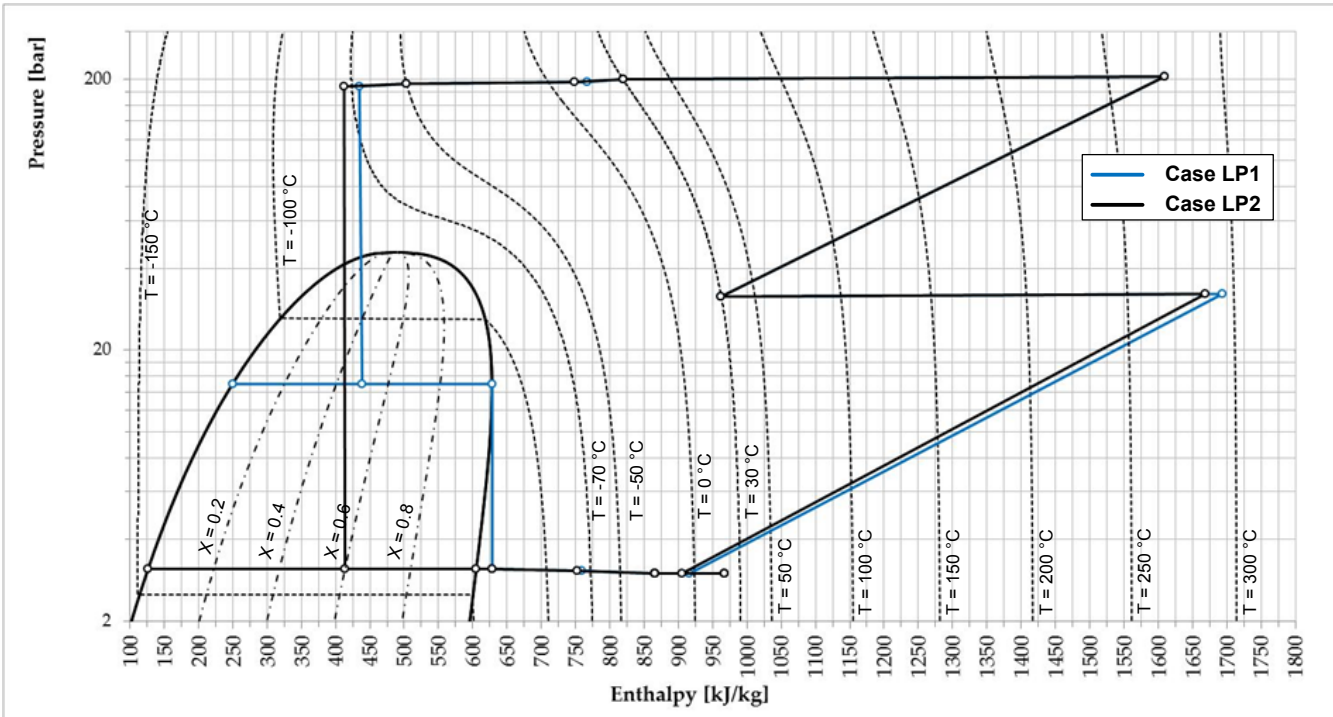

Figure 10 – Thermodynamic diagram of the process obtained for the Case LP1 (blue line) and for the Case LP2 (black line).

The electrical energy results obtained from the analysis of the considered cases are presented in Table 4: these results represent the electric power for each kg/s of LNG produced, thus they can be considered as specific energy. In particular, the total specific electric energy consumption – that is the performance indicator named e, also plotted in Figure 11 – is listed along with the separate contribution of the compression train C1, the compression train C2 and the chiller.

As it can be seen, the case with the lower achieved quality (Case MP2) is also the case with the lower specific electric energy consumption: the introduction of the turbo-expander instead of the throttle valve, indeed, allows to considerably decrease the process consumption, obtaining an electric energy saving of about the 19%. Furthermore, the power produced by means of the expander could be eventually recovered and employed for internal process consumptions, enabling to achieve a decrease in the need of electric energy from the external grid equal to the 24%.

Relating to the low pressure NG grid cases, from the table it can be noted that the total specific electric energy consumption results always higher than the one of the cases with 30 bar at the NG feed-in, even if the compressor in the secondary line has been eliminated. This evidence can be easily explained if considering the different pressure ratios: the maximum pressure of the cycle, indeed, has been maintained constant for all the analyzed cases, thus the compressor's work considerably increases when the inlet pressure passes from a value of 30 bar (Case MP1 and Case MP2) to a value equal to 3 bar (Cases LP1 and LP2). In any case, the consumption increase is lower for the layout with two Joule-Thompson valves (Case LP1), due to the lower quality compared to Case LP2. Furthermore, this trend confirms [44] that high pressure LNG storage allows to improve the performance of the cycle relating to low pressure LNG storage.

In addition, with respect to the usual electric energy consumption of large-scale facilities (equal to about 1200÷1300 kJ/kg$_{LNG}$ [36]), Case MP2 results comparable, while the low pressure configurations have an energy consumption two or three times higher than the large-scale typical one.

Table 4 – Electric energy results of the analyzed cases.

		Case MP1	Case MP2	Case LP1	Case LP2
Compressor 1 electric consumption (P_{C1})	[kJ/kg$_{LNG}$]	1079	885	2795	3485
Compressor 2 electric consumption (P_{C2})	[kJ/kg$_{LNG}$]	209	143	-	-
Chiller electric consumption ($P_{chiller}$)	[kJ/kg$_{LNG}$]	583	479	470	557
Total specific electric consumption (e)	**[kJ/kg$_{LNG}$]**	**1871**	**1506**	**3265**	**4041**
Expander electric production (P_{E1})	[kJ/kg$_{LNG}$]	-	81	-	-
Total net electric consumption	**[kJ/kg$_{LNG}$]**	**1871**	**1425**	**3265**	**4041**

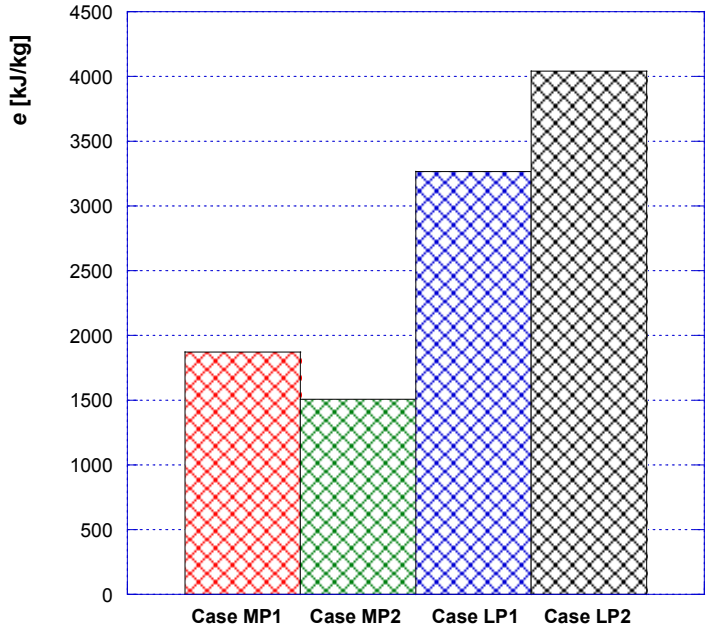

Figure 11 – Total specific electric energy consumption (*e*) of the analysed cases.

For what concerns the thermal energy fluxes of the process, instead, the results are presented in Table 5. Passing from the Case MP1 with the throttle valve to the Case MP2 with the turbo-expander, a decrease in the heat exchanged by both HE1 and HE3 can be seen, thanks to the reduction of the mass flow rate (reduction of the quality). This obtained decrease causes a variation in the temperature level at the inlet of the compressor C2 (*i.e.* T_{14} increases), producing further benefits. Since for Case MP1 the temperature T_{14} results very low (close to the lower limit for the integrity of compressors, reported by the main compressors' manufacturers), indeed, this variation is an important advantage.

Another effect of the increase of the temperature T_{14} is a slight increase in the heat exchanged by the after-cooler AC-C2 for fixed mass flow rate through to be cooled (in the considered cases the mass flow rate through C2 in Case MP2 is lower than in Case MP1, thus the heat exchanged by AC-C2 is almost the same for the two configurations). On the other hand, relating to the compression train C1, the decrease of the inter-cooling and of the after-cooling loads is mainly due to the decreases of the mass flow rate.

As already seen for the electric energy considerations, Cases LP1 and LP2 should be considered separately, in particular regarding the inter-cooler and the after-cooler exchange. The higher mass flow rates and the higher temperature at the end of the first compression stage of C1, indeed, cause the need to remove substantial quantities of heat. The heat exchanged by HE1 and HE3 is comparable with those discussed for the other two cases.

Furthermore, in order to provide more information about the thermal exchange in the heat exchangers HE1 and HE3, in Figure 12 a comparison of the coefficient US (*i.e.* the product between the global heat exchange coefficient U and the exchange surface S) between the analyzed cases is presented. Generally speaking, from a thermodynamic point of view, to have high values of US is a desirable condition: since the coefficient US is expressed in kW/°C, indeed, the higher is US the higher is the heat exchange for a given temperature difference. In the considered analysis several factors contribute to the heat exchange, thus the product US can give an idea of the exchange quality but cannot be considered as a major parameter for the choice of the best performing case.

Table 5 – Thermal energy results of the analyzed cases.

		Case MP1	**Case MP2**	**Case LP1**	**Case LP2**
Q_{HE1}	[kJ/kg$_{LNG}$]	122	79	130	221
Q_{HE3}	[kJ/kg$_{LNG}$]	144	114	106	171
Q_{IC-C1}	[kJ/kg$_{LNG}$]	524	481	1450	1766
Q_{AC-C1}	[kJ/kg$_{LNG}$]	575	508	1542	1941
Q_{AC-C2}	[kJ/kg$_{LNG}$]	105	102	-	-
IC+AC thermal exchange	**[kJ/kg$_{LNG}$]**	**1204**	**1091**	**2992**	**3707**
Total thermal exchange	**[kJ/kg$_{LNG}$]**	**1470**	**1284**	**3228**	**4099**

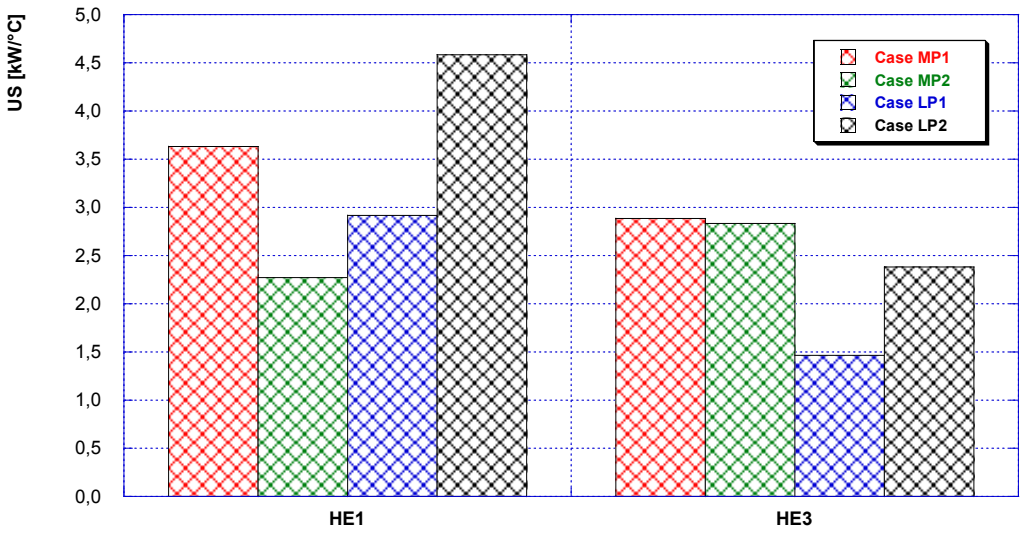

Figure 12 – Comparison of the product US for the heat exchangers HE1 and HE3 in the analyzed cases.

Finally, in Figure 13 and in Figure 14 respectively, the residual lower heating value of the fuel (LHV_R) and the fuel degradation index (ρ) are presented for the analyzed cases. In more detail, for the calculation of LHV_R and of ρ the following assumptions have been made: the reference electrical efficiency ($\eta_{el,ref}$) is supposed to be equal to 0.55 (*i.e.* a typical combined cycle has been considered as reference generation system) and the LHV of the reference fuel has been set equal to 50˙000 kJ/kg (natural gas). Furthermore, it must be highlighted that – relating to Case MP2 – the positive contribute of the expander produced power has not been considered for the indexes calculation, in order to have a comparison between the cases as much as possible under equal conditions.

As it can be seen from the figures, Case MP2 presents the higher values of LHV_R and ρ, thus it is confirmed as the most performing solution between the proposed configurations.

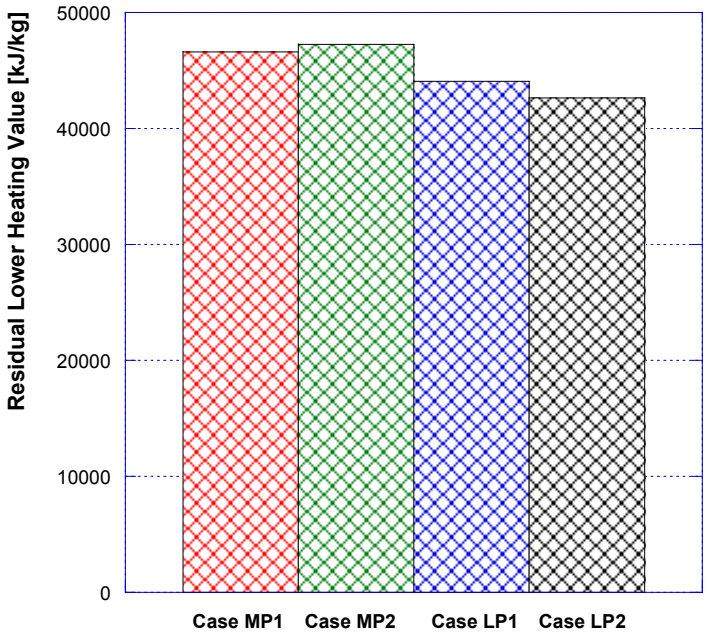

Figure 13 – Residual Lower Heating Value (LHV_R) of the analysed cases.

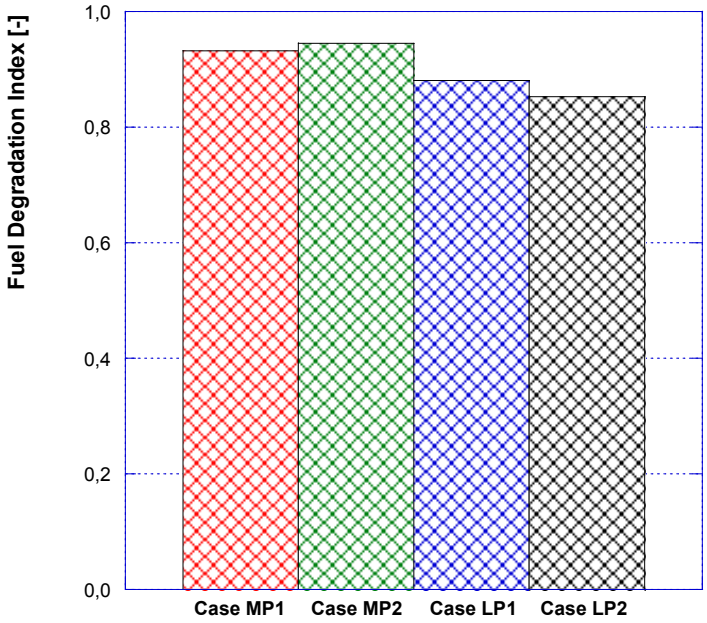

Figure 14 – Fuel Degradation Index (ρ) of the analysed cases.

6. CONCLUDING REMARKS

Since in the next years the global energy demand is expected to continuously grow, fossil fuels are predicted to still play an essential role even if the penetration of renewable energy sources is increasing. In particular, natural gas is the most promising solution – due to its lower environmental impact than other fossil fuels – and LNG can be considered a viable solution for vehicular applications thanks to the reduction of volumes. Currently, the main LNG production plants are located nearby the extraction sites and the LNG is then transported by ship to final users (when no regasification occurs).

In this scenario, this paper aims to define a small-scale configuration to produce LNG at refueling station, in order to be directly used in vehicular sector.

With this purpose four different configurations for LNG production have been proposed: in the Case MP1 the liquefaction is provided by means of a Joule-Thompson valve, while in the Case MP2 by means of a turbo-expander (both these two cases consider a natural gas grid operating with a pressure equal to 30 bar); on the other hand, Case LP – divided into two configurations (Case LP1 and Case LP2) depending on the LNG storage pressure – considers the natural gas grid working at 3 bar. The developed liquefaction configurations have been analyzed with an in-house developed software, in order to determine and compare the processes performance. In particular, various performance indicators have been introduced and applied. Comparing the four developed configurations, the analysis shows that the Case MP2 seems to be the most promising solution, due to its lower specific electric energy consumption (equal to about 1400 kJ/kg_{LNG}, a value comparable with large-scale facilities consumption) and its higher LNG residual lower heating value (equal to around 47˙000 kJ/kg). If considering separately the low pressure cases, instead, the analysis confirms the great influence of the LNG storage pressure on the whole process consumption and fixes the Case LP1 as preferable configuration for low pressure NG supply grids.

Furthermore, the obtained thermodynamic results suggest the need of deep economic analysis which will be the object of future studies.

REFERENCES

[1] The outlook for energy: A view to 2040. http://www.exxonmobil.com/Corporate/Files/news_pub_eo2012.pdf.
[2] World Energy Outlook 2014; International Energy Agency (IEA).
[3] Natural Gas Issues and Trends; U.S. Energy Information Administration (EIA), April 1998.
[4] S. Kumar, H. T. Kwon, K. H. Choi, W. Lim, J. H. Cho, K. Tak, I. Moon. LNG: An eco-friendly cryogenic fuel for sustainable development. Applied Energy 88 (2011) 4264-4273.
[5] S. Gowid, R. Dixon, S. Ghani. Profitability, reliability and condition based monitoring of LNG floating platforms: A review. Journal of Natural Gas Science and Engineering 27 (2015) 1495-1511.
[6] BP Energy Outlook 2035. http://www.bp.com/energy outlook.
[7] A. J. Finn, G. L. Johnson, T. R. Tomlinson. Developments in natural gas liquefaction. Hydrocarb. Process. 1999, 78 (4), 47–59.
[8] D. L. Andress. The Phillips Optimized Cascade LNG Process: a Quarter Century of Improvements. Phillips Petroleum Company: Bartlesville, OK, 1996.
[9] P. Bosma, R. K. Nagelvoort. In: Liquefaction Technology; Developments through History, 1st Annual Gas Processing Symposium, Doha, Qatar, January 10–12, 2009.
[10] P.-Y. Martin, B. Fischer. In: Natural Gas Liquefaction Processes Comparison, 14th International Conference and Exhibition on Liquefied Natural Gas (LNG-14), Doha, Qatar, March 21–24, 2004.
[11] ConocoPhillips Optimized Cascade Process. http://lnglicensing.conocophillips.com.
[12] T. Shukri. LNG Technology Selection. Hydrocarbon Eng. February 2004.
[13] W. Schmidt, B. Kennington. Air Products meets requirements of full range of Floating LNG concepts. LNG J. March 10, 2011.
[14] F. A. Michelsen, I. J. Halvorsen, B. F. Lund, P. E. Wahl. Modeling and Simulation for Control of the TEALARC Liquified Natural Gas Process. Ind. Eng. Chem. Res. 2010, 49 (16), 7389–7397.
[15] A. Singh, M. Hovd. Dynamic Modeling and Control of the PRICO LNG process. In 2006 AIChE Annual Meeting, San Francisco, CA, November 12–17, 2006.
[16] L. K. Swenson. Single mixed refrigerant, closed loop process for liquefying natural gas. U.S. Patent 4,033,735, Jul. 5, 1977.
[17] Y. N. Liu, C. L. Newton. Feed gas drier precooling in mixed refrigerant natural gas liquefaction processes. U.S. Patent 4,755,200, Jul. 5, 1988.
[18] M. Pillarella, Y.-N. Liu, J. Petrowski, R. Bower. The C3MR liquefaction Cycle: Versatility for a Fast Growing, Ever Changing LNG Industry. In 15th International Conference on LNG (LNG-15), Barcelona, Spain, April 24–27, 2007.
[19] P. Y. Martin, J. Pigourier, B. Fischer. LNG process selection, no easy task. Hydrocarbon Eng. May, 2004.
[20] W. Dam, S. M. Ho. Unusual design considerations drive selection of Sakhalin LNG plant facilities. Oil Gas J. October 1, 2001; pp 58–69.
[21] C. L. Newton. Dual mixed refrigerant natural gas liquefaction with staged compression. U.S. Patent 4,525,185, Jun. 25, 1985.
[22] E. Berger, W. Forg, R. S. Heiersted, P. Paurola. The MFC® (Mixed Fluid Cascade) Process for the First European Baseload LNG Production Plant; Linde, 2003.
[23] J. M. van de Graaf, B. Pek. Large-capacity LNG Trains – The Shell parallel Mixed Refrigerant Process. In Business Briefing: LNG Review, 2005.
[24] M. J. Roberts, R. Agrawal. Hybrid Cycle for the Production of Liquefied Natural Gas. U.S. Patent 6,308,531, Oct. 30, 2001.
[25] E. Flesch, J. C. Raillard. CII Liquefaction Process: 2 cascades into 1. In 12th International Conference and Exhibition on Liquefied Natural Gas (LNG-12), Perth, Australia, May 4–7, 1998.
[26] H. Bauer. A Novel Concept for Large LNG Baseload Plants. In 2001 AIChE Spring National Meeting, Houston, TX, April 22–26, 2001.
[27] C. W. Remeljej, A. F. A. Hoadley. An exergy analysis of smallscale liquefied natural gas (LNG) liquefaction processes. Energy, 2006, 31 (12), 2005–2019.
[28] The Kryopak EXP LNG Process. http://www.lngplants.com/KryopakTypicalProcessDescription.html.
[29] K. J. Vink, R. K. Nagelvoort. Comparison of Baseload Liquefaction Processes. In 12th International Conference and Exhibition on Liquefied Natural Gas (LNG-12), Perth, Australia, May 4–7, 1998.
[30] A. J. Finn. Effective LNG Production Offshore. In 81st Annual GPA Convention, Dallas, Texas, March 10–13, 2002.
[31] J. H. Foglietta. Production of LNG using Dual Independent Expander Refrigeration Cycles. In AIChE Spring National Meeting, New Orleans, LA, March 10–14, 2002.
[32] J. H. Foglietta. Consider dual independent expander refrigeration for LNG production. Hydrocarbon Process. January, 2004.
[33] I. B. Waldmann. Evaluation of Process Systems for Floating LNG Production Units. In Tekna Conference, June 18–19, 2008.
[34] P. E. Susan Walther. A new generation of liquefaction processes for LNG FPSO applications. In International Gas Union Research Conference, Paris, October 08, 2008.
[35] T. He, Y. Ju. Optimal synthesis of expansion liquefaction cycle for distributed-scale LNG (liquefied natural gas) plant. Energy, 88 (2015) 268-280.
[36] C. W. Remeljej, A. F. A. Hoadley. An exergy analysis of small-scale liquefied natural gas (LNG) liquefaction processes. Energy, 31 (2006) 2005-2019.
[37] http://www.igu.org/sites/default/files/node-page-field_file/IGURemoteLNG.pdf
[38] T. Kohler, M. Bruentrup, R. D. Key. Edvardsson T. Choose the best refrigeration technology for small-scale LNG production. Hydrocarbon Process, (2014) 45–52.
[39] S. Thomas, R. A. Dawe. Review of ways to transport natural gas energy from countries which do not need the gas for domestic use. Energy, 2003;28 (14):1461–77.
[40] J. Kim, Y. Seo, D. Chang. Economic evaluation of a new small-scale LNG supply chain using liquid nitrogen for natural-gas liquefaction. Applied Energy, 2016;182:154-163.

[41] Z. Yuan, M. Cui, Y. Xie, C. Li. Design analysis of a small-scale natural gas liquefaction process adopting single nitrogen expansion with carbon dioxide pre-cooling. Applied Thermal Engineering 2014;64 (1-2):139-146.
[42] T.B. He, Y.L. Ju. A novel process for small-scale pipeline natural gas liquefaction. Applied Energy 2014;115:17-24.
[43] R. Jokinen, F. Pettersson, H. Saxén. An MILP model for optimization of a small-scale LNG supply chain along a coastline. Applied Energy 2015;138:423-431.
[44] M. A. Ancona, M. Bianchi, L. Branchini, A. De Pascale, F. Melino, M. Mormile, M. Palella. A Novel Small Scale Liquefied Natural Gas Production Process at Filling Stations: Thermodynamic Analysis and Parametric Investigation. Proceedings of ASME Turbo Expo 2016. Seoul, Korea, June 13-17, 2016.
[45] W. Mayzan, A. Ahmadi, H. Ahmed and M. Hoorfar. Market and technology assessment of natural gas processing: A review. Journal of Natural Gas Science and Engineering, 30 (2016) 487-514.
[46] W. Lim, K. Choi, I. Moon. Current Status and Perspectives of Liquefied Natural Gas (LNG) Plant Design. Industrial & Engineering Chemistry Research, 2013, 52 (9), 3065-3088.
[47] L. Ciampitti, C. Marchetti. *Ampliamento stoccaggi gas naturale e produzione LNG*.
[48] www.scania.com
[49] http://www.hvm-li.com/en/index.html
[50] S. Liu, X. Li, Y. Huo, H. Li. An Analysis of the Primary Energy Consumed by the Re-Liquefaction of Boil-Off Gas of LNG Storage Tank. Energy Procedia, 75 (2015) 3315-3321.
[51] Y. Li, X. Wang, Y. Ding. An optimal design methodology for large-scale gas liquefaction. Applied Energy, 99 (2012) 484-490.
[52] P. Colonna and T. P. Van der Stelt. FluidProp: A program for the estimation of thermophysical properties of fluids. software, 2004. http://www.asimptote.nl/software/fluidprop.
[53] Snam rete gas – Italian national natural gas transportation leader. http://misura.snam.it/portmis/coortecDocumentoController.do?menuSelected=4300
[54] T.E. Rufford, S.Smart, G.C.Y.Watson, B.F.Graham, J.Boxall, J.C.DinizdaCosta, E.F.May. The removal of CO_2 and N_2 from natural gas: A review of conventional and emerging process technologies. Journal of Petroleum Science and Engineering, 94-95 (2012) 123-154.

APPENDIX A

Table A1 – Physical conditions and mass flow rates in each section of the process – Case 1.

Plant Section	Mass Flow Rate [kg/s]	Temperature [°C]	Pressure [bar]	Quality [-]
1	1.00	20	30.0	-
2	2.04	25	30.0	-
3	2.04	-5	29.4	-
4	2.04	122	94.5	-
5	2.04	30	92.7	-
6	2.04	118	203.9	-
7	2.04	30	200.0	-
8	2.04	-50	196.0	-
9	2.04	-65	192.2	-
10	2.04	-115	15.0	0.510
11	1.00	-115	15.0	0
12	1.04	-115	15.0	1
13	1.04	-71	14.7	-
14	1.04	-11	14.4	-
15	1.04	22	20.2	-
16	1.04	22	19.7	-
17	1.04	71	30.6	-
18	1.04	30	30.0	-

Table A2 – Physical conditions and mass flow rates in each section of the process – Case 2.

Plant Section	Mass Flow Rate [kg/s]	Temperature [°C]	Pressure [bar]	Quality [-]
1	1.00	20	30.0	-
2	1.67	24	30.0	-
3	1.67	-5	29.4	-
4	1.67	133	94.5	-
5	1.67	30	92.7	-
6	1.67	125	203.9	-
7	1.67	30	200.0	-
8	1.67	-50	196.0	-
9	1.67	-62	192.2	-
10	1.67	-115	15.0	0.403
11	1.00	-115	15.0	0
12	0.67	-115	15.0	1
13	0.67	-71	14.7	-
14	0.67	2	14.4	-
15	0.67	92	30.6	-
16	0.67	30	30.0	-

Table A3 – Physical conditions and mass flow rates in each section of the process – Case 3a.

Plant Section	Mass Flow Rate [kg/s]	Temperature [°C]	Pressure [bar]	Quality [-]
1	1.00	20	3.0	-
2	1.99	-3	3.0	-
3	1.99	295	32.2	-
4	1.99	30	31.6	-
5	1.99	275	203.9	-
6	1.99	30	200.0	-
7	1.99	15	196.0	-
8	1.99	-50	192.2	-
9	1.99	-67	188.4	-
10	1.99	-115	15	0.498
11	1.00	-115	15	0
12	0.99	-115	15	1
13	0.99	-136	3.12	-
14	0.99	-76	3.06	-
15	0.99	-26.5	3.0	-

Table A4 – Physical conditions and mass flow rates in each section of the process – Case 3b.

Plant Section	Mass Flow Rate [kg/s]	Temperature [°C]	Pressure [bar]	Quality [-]
1	1.00	20	3.0	-
2	2.50	-8	3.0	-
3	2.50	287	32.2	-
4	2.50	30	31.6	-
5	2.50	275	203.9	-
6	2.50	30	200.0	-
7	2.50	10	196.0	-
8	2.50	-50	192.2	-
9	2.50	-73	188.4	-
10	2.50	-146	3.12	0.601
11	1.00	-146	3.12	0
12	1.50	-146	3.12	1
13	1.50	-79	3.06	-
14	1.50	-26.5	3.0	-